Measurement of low AC currents by the standard current probe equipped with lock-in amplifier

Jiri Svarny
Dept. of Materials and Technology
University of West Bohemia
Pilsen, Czech Republic
svarny@fel.zcu.cz

2022 International Conference on Diagnostics in Electrical Engineering (Diagnostika) | 978-1-6654-8082-6/22/$31.00 ©2022 IEEE | DOI: 10.1109/Diagnostika55131.2022.9905091

***Abstract*—Most of standard current probes are intended for the measurement of medium or higher currents. Usually, due to limited dynamic range, characteristic sensitivity and inner noise of the probe, it is hardly possible to measure currents lower than 100 mA. The paper deals with the possibility to extend the dynamic range of the current probe by an additional external lock-in amplifier. The paper describes the principle of the lock-in amplifier in general and design of the laboratory fixture of lock-in amplifier based on AD630 circuit as well. The designed amplifier was used to condition the output of the Agilent1146A current probe. The experiment is described in detail. The results show that thanks to the lock-in amplifier the currents even lower than 1 mA can be easily detected.**

Keywords—current probe, lock-in amplifier, dynamic range, current measurement, noise suppression

I. Introduction

The current probe is a very useful tool for measurement of electrical current. Usually, it is used as an accessory of common measuring instruments like oscilloscopes or digital multimeters. One of its advantages is galvanic isolation between the measuring instrument and the device under test.

Various types of current probes exist in regard to their principle. There can be found current transformer based probes, Hall sensor based probes or Rogowski coil based probes. The used principle strongly affects the probe features including sensitivity, dynamic range, frequency range, etc. Some probes are based on hybrid design using a combination of various principles to improve particular features. Very common one is the design using combination of current transformer principle and Hall effect sensor principle. In that case it is possible to achieve wider frequency range in comparison to the simple Hall effect sensor based design.

Most of the current probes are optimized for measurement of rather higher currents. The measuring ranges are usually in units or tens of amps. This leads to limited output/input ratio which is used to be in range of hundreds of mV/A at most. The parameter that limits measurement of lower primary current values is output voltage noise of the probe. Usually, there is hardly possible to detect currents lover than 100 mA using a common current probe due to the probe output noise.

In case the noise is truly stochastic, there should exist possibility to suppress the noise by means of a special - phase sensitive amplifier i.e. so called lock-in amplifier (LIA). Advantageously, these amplifiers are sometimes used to condition outputs of various types of sensors in case the massive noise is present. As a specific example of the application there can be mentioned a measurement of weak magnetic fields [1], a measurement of resistance and capacity [2], [3] or a gas detection [4], [5].

The experiment described in this paper discovers how it is possible to enlarge the dynamic range of the current probe and thus allow to measure lower currents by means of simple lock-in amplifier. For needs of the experiment the common current probe Agilent 1146A was used. The probe itself covers the frequency range from DC up to 100 kHz (-3 dB). Two current ranges are available. In case of range 100 mA_{peak} to 10 A_{peak} the output/input ratio is 100 mV/A. In case of range 1 A_{peak} to 100 A_{peak} the output/input ratio is 10 mV/A. It is clear that for the measurement of lower currents the lower range is more suitable. The datasheet of Agilent 1146A states 3 mV output noise voltage for lower range (100 mV/A) [6]. As a result the currents lower than 30 mA are completely masked by the probe noise level and thus unmeasurable using standard output signal conditioning.

II. Lock-in Amplifier – the Principle

The LIA is an circuit that is able to extract amplitude and phase of the input signal even if the signal is buried in the massive noise. The device requires a reference signal with precisely defined frequency that is synchronous with measured signal to work properly. The principle of the LIA is based on the phase sensitive detector (PSD). The standard LIA core consists of two PSDs and single 90° phase shifter. Each of the two PSDs includes one multiplier and one low pass filter (LPF).

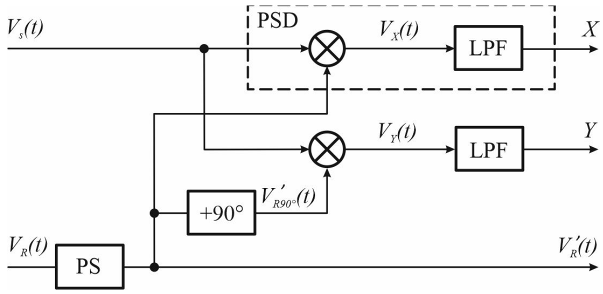

Fig. 1. Lock-in amplifier principle

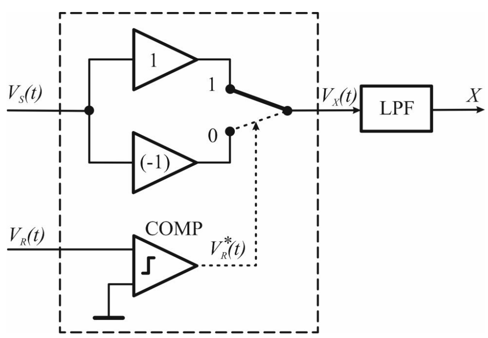

Fig. 2. Switching PSD

Let us consider the $V_S(t)$ sinus input signal of V_S RMS value, f_S frequency and φ_S phase shift. Simultaneously, there is available $V_R(t)$ sinus reference signal of 1 V RMS value and f_R frequency. By means of PS (variable phase shifter) it is possible to adjust the phase shift of the input reference to obtain the $V_R'(t)$ signal (inner reference of the X branch shifted by φ_R). Thanks to the 90° phase shifter (+90° block), there is also produced $V_{R90}'(t)$ reference signal (inner reference of the Y branch shifted by $\varphi_R + 90°$). Usually, the reference frequency is equal to the frequency of measured signal ($f_S = f_R$). The outputs of the multipliers will generate signals combined of DC and AC components. For further analysis the AC components are useless. On the other hand, the DC components carry valuable information about the measured signal. The AC components can be easily filtered out using the LPFs. The X and Y outputs hold the desired DC levels then. The RMS value and the phase shift between the measured signal and the reference can be calculated from X and Y as follows:

$$V_S = \sqrt{X^2 + Y^2}\ ,\ \ \varphi_S - \varphi_R = arctan\frac{Y}{X} \qquad (1)$$

The detail derivation of (1) can be found in [7] or [8] for instance. Generally, the sinus waveform of the reference is not necessary. The rectangular reference is also applicable. Advantageously, in that case the PSD implementation can be simplified. The precise analog multipliers can be substituted by simple electronic switches to alternate the polarity of the input signal. Such a PSD is called the switching PSD then. The implementation of the LIA X branch using the switching PSD is depicted in Fig. 2. As a practical example of such a design can be mentioned [9].

The $V_R^*(t)$ unit reference signal with f_R frequency can be described as follows:

$$V_R^*(t) = 1 \quad \text{for} \quad t \in \left(0;\ \frac{1}{2f_R}\right)$$

$$V_R^*(t) = -1 \quad \text{for} \quad t \in \left(\frac{1}{2f_R};\ \frac{1}{f_R}\right)$$

resp.

$$V_R^*(t) = \frac{4}{\pi}\sum_{k=1}^{\infty}\frac{1}{k}sin(k\omega t)\ ;$$

$$\omega = 2\pi f_R;\ \ k = 2n - 1 \qquad (2)$$

Let us consider the $V_S(t)$ measured signal of sinus waveform, the V_S RMS level, the frequency f_S which is the same as reference one ($f_S = f_R$) and φ phase shift related to the reference

$$V_S(t) = \sqrt{2}V_S sin(2\pi f_S t + \varphi) \quad . \qquad (3)$$

At the output of the switch we achieve $V_X(t)$ signal.

$$\begin{aligned} V_X(t) &= V_R^*(t)\cdot V_S(t) = \\ &= V_S\sqrt{2}\frac{2}{\pi}[cos(\varphi) - cos(2\omega t + \varphi)] + \\ &+ V_S\sqrt{2}\frac{2}{\pi}\sum_{k=3}^{\infty}\frac{1}{k}\{cos[(1-k)\omega t - \varphi] - \\ &- cos[(1+k)\omega t + \varphi]\} = \\ &= V_S\sqrt{2}\tfrac{2}{\pi}\cos(\varphi) + AC\ comp. \end{aligned} \qquad (4)$$

The LPF is designed to cut off all the AC components (AC comp.) of $V_X(t)$ signal. Only the DC level of the $V_X(t)$ signal will appear at the X output

$$X = V_S\sqrt{2}\tfrac{2}{\pi}\cos(\varphi) \qquad (5)$$

In case the $V_R^*(t)$ is shifted by 90° (or better to say by the using of second PSD) we would obtain quadrature output Y instead of X one

$$Y = V_S\sqrt{2}\tfrac{2}{\pi}\sin(\varphi) \qquad (6)$$

The X and Y outputs can be used to recon the measured level and phase shift regard to the reference the same way as in case of standard LIA structure

$$\begin{aligned} &\sqrt{X^2 + Y^2} = \\ &= \sqrt{\left(V_S\sqrt{2}\frac{2}{\pi}\right)^2 cos^2(\varphi) + \left(V_S\sqrt{2}\frac{2}{\pi}\right)^2 sin^2(\varphi)} = \\ &= \sqrt{\left(V_S\sqrt{2}\tfrac{2}{\pi}\right)^2 [cos^2(\varphi) + sin^2(\varphi)]} = V_S\sqrt{2}\tfrac{2}{\pi} \end{aligned} \qquad (7)$$

$$\frac{Y}{X} = \frac{V_S\sqrt{2}\frac{2}{\pi}sin(\varphi)}{V_S\sqrt{2}\frac{2}{\pi}cos(\varphi)} = tan(\varphi) \quad \Rightarrow \quad \varphi = arctan\frac{Y}{X} \qquad (8)$$

III. Lock-in Amplifier Design

If the $V_S(t)$ signal is in phase with $V_R(t)$, the quadrature component i.e. the level at the Y output will always stay zero. Overall the quadrature branch is useless and can be omitted in that case. The LIA can be simplified and implemented by means of single PSD then. The signal at the X output will be proportional to the V_{Sm} amplitude of the measured signal

$$X = \sqrt{2}V_S\tfrac{2}{\pi} = V_{Sm}\tfrac{2}{\pi} \quad . \qquad (9)$$

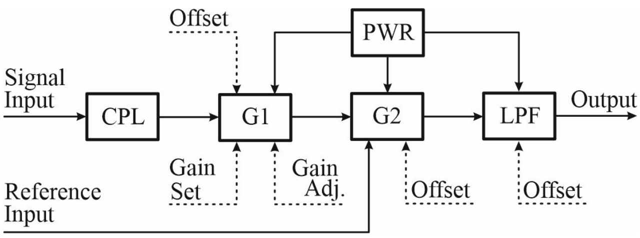

Fig. 3. Block diagram of the designed LIA

This is the case of the implemented LIA as well. The design of the experimental LIA was based on single AD630 [10] integrated circuit and two AD711 precision operational amplifiers. The measured signal is lead to the input of the first AD711. This stage is designed as the non-inverting preamplifier with G_1 gain. The G_1 gain is variable and can be set to 1, 5 or 50. The input coupling is defined by CPL block and can be set to AC or AC+DC. In case of the AC couple the lower frequency margin is 0.1 Hz. Next stage is implemented by AD630. The gain of this stage is set to $G_2 = \pm 2$. The polarity of the G_2 gain is switched by the inner comparator of the AD630 that is controlled by reference signal. The last stage is formed by the Sallen-Key LPF. The upper corner frequency is 1 Hz approximately. The filter is implemented by second AD711 operational amplifier. Each stage is equipped with the offset compensation. The overall gain of the LIA is defined by (10). If the maximum gain of the preamplifier stage is chosen the output level of the LIA is defined as follows

$$X = G_1 |G_2| \sqrt{2} V_S \frac{2}{\pi} = V_{Sm} \frac{200}{\pi} \tag{10}$$

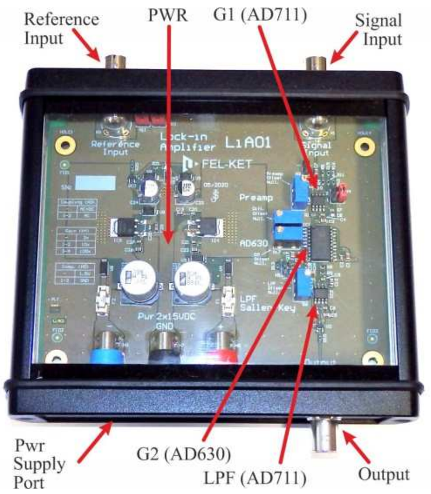

Fig. 4. The designed LIA fixture

IV. Experiment

The designed LIA was connected to the output of the Agilent 1146A current probe. The probe was switched to 10 A range and zeroed. The measured current was generated by Keysight 33506B function generator. The generator was loaded by the R_L resistor of 50 Ω nominal value. The probe was clipped around the one of the R_L resistor leads. The generator reference output was connected directly to the LIA reference input. The output voltage of the LIA was measured by Escort 3136A multimeter. The primary current was measured indirectly as a voltage drop across the R_L load resistor by Agilent 34401A multimeter. The DSOX2002A oscilloscope was used to monitor the output signal of the current probe and reference signal as well. The overall arrangement is depicted in Fig. 5.

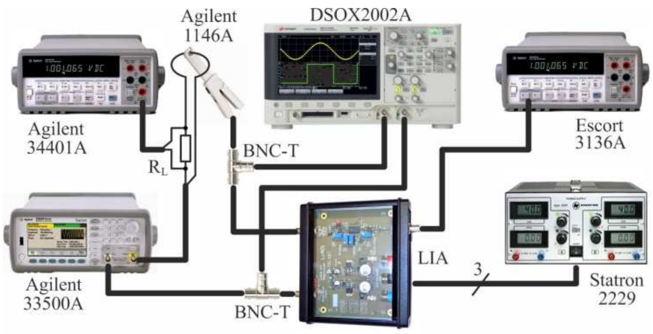

Fig. 5. The arrangement of the experiment

There was chosen 1 kHz sinus output at the generator. The output level was adjusted in order to achieve desired measured current I_{SRMS} (i.e. needed U_{SRMS} voltage drop across the R_L load resistor). The precise value of the R_L has been measured as 50.713 Ω before. The primary current was varied from 50 mA down to 0.1 mA RMS. The Fig. 6. discovers the shape of the output signal of the probe for various measured levels. It is obvious that in all the cases the waveform is significantly affected by the noise. The direct measurement of the 50 mA level is possible with certain difficulties. In case of lower values (5 mA, 0.5 mA) the direct measurement is entirely impossible as the signal is completely buried in the noise.

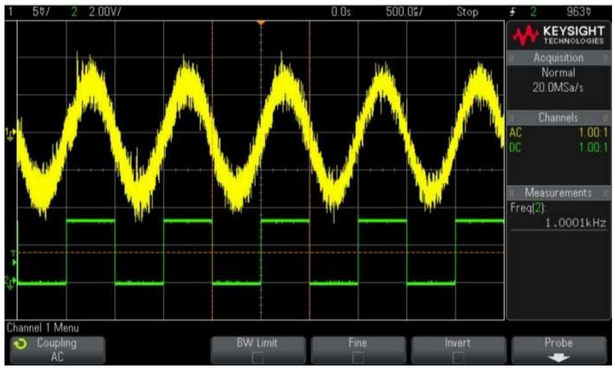

a)

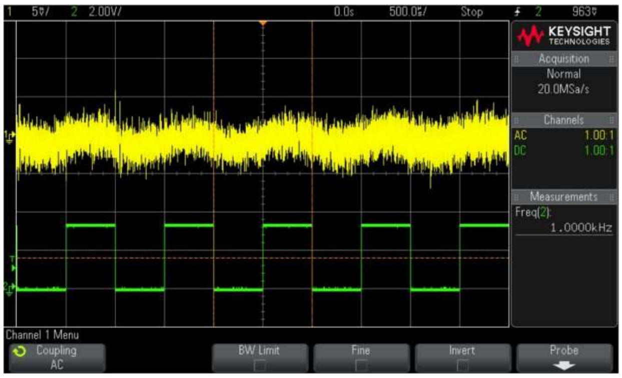

b)

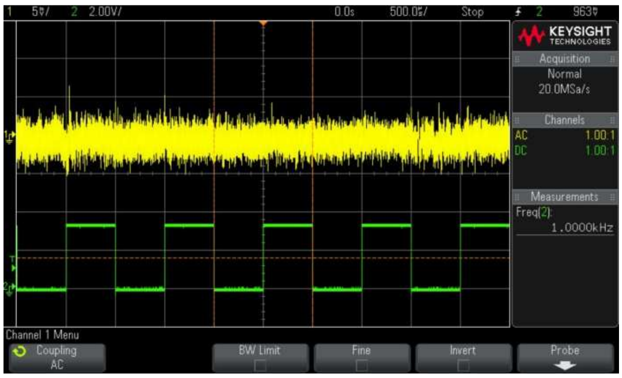

c)

Fig. 6. The Agilent 1146A current probe output for various measured levels: a) 50 mA RMS, b) 5 mA RMS, c) 0.5 mA RMS (yellow track). The reference signal is represented by the green track.

V. Results

In the experiment there were compared the RMS values detected by the measurement (I_{RRMS}) with the RMS values of current being set (I_{SRMS}). As the measured value was decreased lower and lower, the relative fluctuation of the LIA output increased. This is the natural feature given by the design of the LIA (especially by the design of LPF stage). The fluctuation of ±5 % related to the average value was chosen as the limit criterion of the output relevance. The fluctuation of the LIA output was always tested for 1 minute. During this period there was tested and stored the minimum and maximum of the LIA output (V_{omin}, V_{omax} values respectively) using the special Min/Max function of the Escort 3136A multimeter. The approximate average value V_o

was calculated by averaging of V_{omax} and V_{omin} values. The relative level of fluctuation was calculated as follows

$$\delta = \frac{\Delta}{V_O}100 = \frac{\frac{V_{omax}-V_{omin}}{2}}{\frac{V_{omax}+V_{omin}}{2}}100 = \frac{V_{omax}-V_O}{V_O}100 \qquad (11)$$

The V_o value, the known gain of the LIA (G_A coefficient) and the output/input ratio of current probe (S_P coefficient) were used to calculate the measured current I_{RRMS}.

$$I_{RRMS} = \frac{G_A V_o}{S_P} = \frac{\pi V_o}{200 S_p \sqrt{2}}$$

$$\text{where} \quad S_P = 100\, mV/A \qquad (12)$$

All the measured and calculated data can be found in Table I.

TABLE I. MEASURED DATA

I_{SRMS} (mA)	V_{SRMS} (V)	V_{omax} (mV)	V_{omin} (mV)	V_o (mV)	δ (%)	I_{RRMS} (mA)
50	2.5357	455.81	455.30	455.56	0.06	50.598
25	1.2678	228.09	227.63	227.86	0.10	25.310
10	0.5071	91.55	90.97	91.26	0.32	10.136
7.5	0.3804	68.76	68.23	68.50	0.39	7.608
5	0.2536	45.93	45.42	45.68	0.56	5.073
2.5	0.1268	23.28	22.64	22.96	1.39	2.550
1	0.0507	9.48	8.90	9.19	3.16	1.021
0.75	0.0380	7.24	6.61	6.93	4.55	0.769
0.5	0.0254	4.97	4.42	4.70	5.86	0.521
0.25	0.0127	2.69	2.08	2.39	12.79	0.265
0.1	0.0051	1.32	0.79	1.06	25.12	0.117

The measured data were depicted in charts. The chart in Fig. 7 represents dependency of measured current (I_{RRMS}) on the set value (I_{SRMS}). The transmission characteristic is linear and the approximation (red line) only slightly differs from the ideal shape (blue line). There was detected offset of 0.012 mA and gain error of 1.2 % only. The Fig. 8 shows the dependency of the level of the relative fluctuation (δ) on the set current (I_{SRMS}). The chart reveals that for the ±5 % criterion of maximum acceptable fluctuations the lowest measurable current is 0.6 mA RMS.

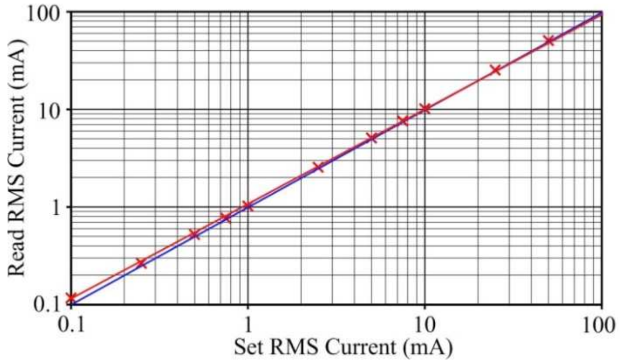

Fig. 7. Transmission characteristic – the dependency of measured value on the set value (measured values – red crosses, linear approximation of measured values – red line, ideal shape – blue line).

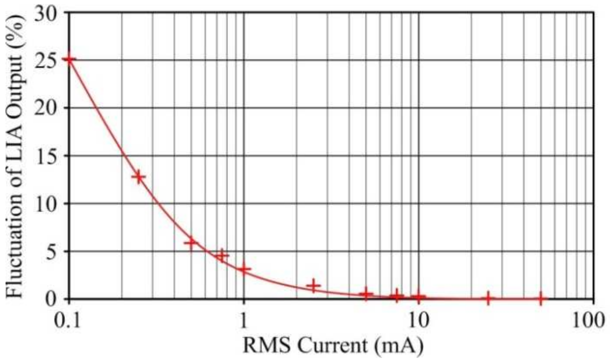

Fig. 8. Dependency of relative fluctuations on the measured current

VI. CONCLUSION

The experimental LIA fixture was successfully designed and tested. The LIA was implemented as a device to condition output of the Agilent 1146A current probe. The transmission chart of the measuring chain is highly linear. The results demonstrate very small offset and gain error in comparison to ideal shape of transmission characteristics. Moreover, both the negligible imperfections can be suppressed further by a more precise adjustment of the LIA set-up. Thanks to the LIA, the dynamic range of the standard current probe was significantly extended. Due to the output noise the probe itself is hardly applicable for trustworthy measurement of currents lower than 100 mA approximately. When the probe was equipped with the proposed LIA there was possible to detect currents even lower than 1 mA. It is supposable, that more sophisticated design of the LIA could improve the sensitivity of the measuring chain even further.

REFERENCES

[1] Hengli Song, Haobin Dong and Lin Zhang, “Application of lock-in amplifier to weak magnetic field detection,” Int. Conf. on Mechatronics, Electronic, Industrial and Control Engineering (MEIC), pp. 1092-1096, 2014.

[2] K. G. Libbrecht, E. D. Black and C. M. Hirata, “A basic lock-in amplifier experiment for the undergraduate laboratory,” American Journal of Physics, vol. 71, issue 11, pp. 1208-1213, October 2003.

[3] P. Maya, B. Calvo, M. T. Sanz-Pascual and J. Osorio, “Low cost autonomous lock-in amplifier for resistance/capacitance sensor measurements,” Electronics, vol. 8, issue 12, November 2019.

[4] P. M. Maya-Hernandez, L. C. Alvarez-Simon, M. T. Sanz-Pascual and B. Calvo-Lopez, “An integrated low-power lock-in amplifier and its application to gas detection,” Sensors, vol. 14, August 2014.

[5] A. De Marcellis, G. Ferri, A D’ Amico, C. Di Natale and E. Martinelli, “A fully-analog lock-in amplifier with automatic phase alignment for accurate measurements of ppb gas concentrations,” IEEE Sensors J., vol. 12, no. 5, pp. 1377-1383, May 2012.

[6] Keysight Corp., “Infinii vision oscilloscope probes and accessories for 1000 X-, 2000 X-, 3000A/T X-, 4000 X-, 6000 X-, 5000, 6000, and 7000 Series,” Selection Guide, Available on-line: www.keysight.com

[7] Sabyasachi Bhattacharyya, Ragib Nasir Ahmed, Basab Bijoy Purkayastha, Kaustubh Bhattacharyya, “Implementation of digital lock-in amplifier,” J. of Physics: Conf. Series, October 2016.

[8] S. DeVore, A. Gauthier, J. Levy and C. Singh “Improving students’ understanding of lock-in amplifiers,” American J. of Physics, vol. 84, Issue 1, 2016.

[9] M.Gabal, N.Medrano, B.Calvo, P.A.Martínez, S.Celma and M.R.Valero, “A complete low voltage analog lock-in amplifier to recover sensor signals buried in noise for embedded applications,” Proc. Eurosensors XXIV, Linz, Austria, September 2010.

[10] Analog Devices Corp., “Balanced Modulator/Demodulator AD630,” Data Sheet, 2016, Available on-line: www.analog.com